Electronic Supplementary Material (ESI) for Lab on a Chip.
This journal is © The Royal Society of Chemistry 2016

A Portable and Reconfigurable Multi-Organ Platform for Drug Development with Onboard Microfluidic Flow Control

J.R. Coppeta[1], M.J. Mescher[1], B.C. Isenberg, A.J. Spencer, E.S. Kim, A.R. Lever, T.J. Mulhern, R. Prantil-Baun, J.C. Comolli and J.T. Borenstein
Materials and Microfabrication Directorate, Draper, Cambridge MA 02139

1 These authors contributed equally.

Supplement Information

Overall Description

As described in the main article, a six-module fluidic circuit, duplicated to form two parallel circuits on the plate, can either create a biological replicate if using the same flow patterns and modules or, alternatively, two different experiments by programming the two systems differently. The schematic in Figure 1s illustrates how pump chambers, valves and fluid paths are configured to mimic complex multi-organ circulatory interaction, specifically with open-well modules, utilizing both inlet and outlet pumps and a robust means for maintaining fluid volume control within modules which can be particularly challenging in a multi-pump open module system. Typical media volumes for each module are shown in Table 1s. The platform technology presented here can be adapted to closed organ models, reducing the dilution ratios shown in Table 1s significantly. Fluid volume in the connecting channels in the platform does not significantly increase the dilution ratios, as the dead volume has been minimized in this system, and further reductions in dead volume for a platform with closed microfluidic organ models are achievable. A mixing reservoir is connected to intake and outlet pumps to distribute fluid between the modules. This design allows future experiments connecting up to five unique tissues (Fig. 2s) while simultaneously testing mixing rates on the individual airway modules herein.

Pump and Valve Description

Pump stroke volume versus pressure, flow rate versus frequency and stroke volume stability data are provided Figures 3s, 4s and 5s, respectively. Below we include detailed descriptions of the pumps and valves.

1) The actuators are assembled on a printed circuit board (PCB). They produce displacement of a small plastic pin normal to and through the PCB plane. A small coil spring produces a zero-power position of the pin. When current is applied to a coil, the annular electromagnet overcomes the spring force and pulls the pin into a recessed position within the PCB (see Figure 2D). The actuators are approximately 7mm in diameter and 2mm in height, and are typically placed at a minimum spacing of 9mm. They produce magnetic forces that range from 1 to 10N, depending on current applied and gap between the two pole faces. The displacement range is approximately 0.2 mm. These performance characteristics were selected to provide sufficient displacement and force to actuate the tensioned polyimide valve and pump structures.
2) The pump chambers are short cylindrical chambers with primary axis placed coincident with the displacement axis of an actuator. Inlet and outlet channels are present on the circumferential face of the chamber, typically with a minimum angular spacing of 45 degrees. A circular membrane forms the top cover of the chamber and serves as the actionable component. It is in contact with the actuator pin through a secondary elastomer layer that distributes localized forces and thus improves membrane fatigue limits. The chamber volume is minimized in the actuator's unpowered state when its coil spring produces a load which displaces the circular membrane into the chamber until either it reaches the chamber bottom or the membrane's elastic restoring force equals that of the coil spring. This action serves as the pumps dispense stroke. With actuator excited, the coil spring

force is magnetically overcome, and the elastic membrane returns to its nominal flat position, maximizing the chamber volume, which serves as the pump's intake stroke. Typical chamber designs include membrane diameter range of 3 to 4.5mm and lengths from 100 to 300um, with nominal dimensions of 4.0mm by 150um. Volumetric displacements, or stroke volumes, can range from 0.1 to greater than 1uL, with a typical design value of 0.6uL.

3) The valves are formed in the same layers as those used for the pump chambers. The valve membranes are typically smaller in diameter (2.8 to 3.3mm) than their pump chamber counterparts to reduce their fluidic compliance which would otherwise degrade pumping performance. In the open state (current applied to the actuator coil), the valve membrane is flat and suspended approximately 100um above an annular elastomeric valve seat. When unpowered, the coil spring and pin deflect the membrane until it seals against the valve seat as shown in Figure 2D. Finally, the valves can provide any typical valve function: valves in parallel can select between multiple inlet or outlet lines, or they can be configured with pump chambers to form multi-directional pumps as described below.
4) The valves and pump chambers can function in sequence to produce pumping. In a typical configuration, a minimum of two valves have direct fluidic connection to a pump chamber. These valves also have a minimum of one connection to another fluid-containing component, e.g. tissue-containing or drug-containing reservoirs. In the first (intake) step of the pumping sequence, one valve is held open (power ON) while the pump chamber expands in volume (power ON). After pump chamber expansion is complete, the inlet valve is closed (power OFF) and the outlet valve is opened (power ON). The pump chamber then decreases in volume (power OFF), which expels fluid through the outlet valve. The sequence is then repeated. Exchanging the electronic timing signals on the valves reverses the direction of flow. For pumps with more than two valves, numerous operational modes are possible. For example, with a three-valve pump, one can distribute an inlet stream in any desired ratio to two outlet channels by duty-cycling the outlet valves.

Actuator Power, Duty Cycle and Temperature Control

In this section, information on energy and power consumption, duty cycle, and the performance of the platform in maintaining and controlling temperature is provided. This data is presented for standard operating protocols; under various operating conditions these numbers may differ, but the following provides a useful baseline for typical platform operation.

1) Energy and power consumption: For a single actuator in a standard pump sequence, (1.1msec spike, 22msec hold open time), the energy required is 34mJ. For a single pump (comprising 3 actuators, one for the pump, and one each for the inlet and outlet valve) running at approximately 1.7Hz (0.6 mL stroke volume, flow rate of 1 mL/sec), each actuator is on for approximately 22 msec, corresponding to a duty cycle D = 22/600 = 3.7%. Another way of characterizing the power consumption is to invoke the metric of power per flow rate delivered. This value is typically on the order of 170mW/(mL/sec), with linear scaling. This translates to a power of 85mW required to drive 0.5 mL/sec. It is important to note that this power/flow rate efficiency level assumes no selector valve is open (as in a self-circulation mode.) In a typical interaction mode (where one selector valve is open), the power per flow rate delivered would be 230mW/(mL/sec). In a less common instance, two selector valves might be open simultaneously. In order to produce a net flow in and out of module, both infuse and withdrawal pumps would have to run, and typically the withdrawal pump would be overbiased by about 40%. Thus in interaction mode, the typical efficiency would be (assuming 1 selector valve) (1+1.4)*230 = 544mW/(μL/sec) for a net flow throughput of a module.
2) Duty Cycle: For a typical use case, the system duty cycle can be characterized as shown in Table 2s, where operational parameters such as the media volumes, interaction and self-circulation volumes and flow rates, and interaction and interaction cycle volumes are provided. In this typical use case presented, the total interaction volume is 10 mL/day. For the total power for this use case the average power is 0.6 W (0.51 W for self-circulation and 0.09 W for interaction).

3) Temperature Control: The actuators driving flow in this platform generate heat that increases temperature during operation in the incubator, necessitating the use of active cooling to maintain an average temperature of 37 C and to minimize gradients across the platform during normal operation. Without active cooling, the temperature rise can be as much as 2 – 3 C, but with active cooling, temperature rise and gradients are generally limited to 0.5 – 1.0 C. A typical method for mitigating this temperature rise is to operate the incubator at 36 C while monitoring local temperature to insure that gradients are maintained within acceptable limits. Tighter control over temperature gradients is possible, but the precision of the temperature sensors must be accounted for in the analysis.

Module Descriptions

Module Descriptions

Each human tissue construct requires a well-controlled microenvironment of unique biological, chemical, and mechanical cues to create organized tissue structures that interact within a tissue scaffold and module to induce the correct differentiation and function of cell types present. Open format tissue modules were designed to demonstrate the feasibility of using commercially available 3D organotypic tissue models. The liver module comprises a machined polymer scaffold with through-holes permitting hepatocyte attachment, culture and media perfusion. A transwell airway tissue model was selected to demonstrate a barrier tissue and a hepatocyte tissue model was selected to demonstrate a perfused tissue [34]. A circulatory module was included to mimic the blood or circulatory compartment. Modules were designed with the following criteria; plug and play functionality allowing individual modules to be arranged arbitrarily in one of the twelve module locations on the fluidic plate, fluidic ports supporting two independent fluidic paths within a module, scaffold mating features to locate the scaffold within a module, low drug sorption materials of construction, compatible with conventional sterilization techniques, easily accessible for manual sampling via a pipette, stable volume control within an open format module, and designs that can be fabricated using conventional machining or injection molding. Figure 6s shows the liver, airway, and circulatory modules designed using the above criteria.

Referring to Figure 1s, the module dimensions are 40 x 22 x 20 mm and are constructed of Class VI polysulfone material (such as USP 1000 from Professional Plastics, Fullerton CA) using conventional machining techniques. These module dimensions are large enough to accommodate several times the surface area and volume of the tissue models selected for demonstration herein. In vitro tissue scaling is a rapidly developing field without a clear consensus on a universal approach with some authors suggesting a functional scaling approach as opposed to a traditional allometric approach [11]. Given the goal of our biologic demonstration was to show viability of interacting organs on the microfluidic system, attempts were not made to scale the liver and lung tissue to either a functional or allometric physiologic model. The tissue mass and media volumes were developed previously in isolation prior to introduction on platform and are described below in section X. In the liver module, hepatocyte cells are supported by a combination of a permanent scaffold machined into the module (label 4 in Figure 1s) and disposable scaffold (not shown). Tracheal bronchial airway cells are supported on a Corning 24-well Transwell 0.4 μm polycarbonate scaffold as shown in Figure 1s. Maximum module media capacities are 4 ml, 4 ml, and 5 ml for the liver, airway, and circulatory modules respectively, but smaller media volumes are typically used in operation (See Table 1s.) Numerical simulations using the Fluid Mechanics module of COMSOL aided the module design and were used to quantifying the intra-module mixing times and to ensure there are no stagnation regions in the flow field. Unless a specific use case dictates otherwise, it is generally desirable to select intra-module pump rates that create well mixed assumptions to apply within the modules at all time scales of interest. This is important for two reasons. First, the system dynamics

should be significantly faster than the biological time scales of interest to mimic the relevant biology. Second, satisfying well mixed assumptions within the modules makes numerical simulations of the system tractable using pharmacokinetic modeling. The intra-module mixing times for the purposes of this demonstration were set to less than one hour. Numerical simulations suggest a bolus introduction of a tracer at the modules' inlet achieved greater than 90% of the steady concentration across the tissue interface for each module after approximately two volume changes for the flow rate range investigated (0.1 to 1 µL/s) and the pump rates were set accordingly to achieve two volume changes within 1 hour. All flows are laminar ($Re_{max} < 10$) and are convectively dominated at the media-tissue interface (Pe> 100) for the conditions investigated herein. Faster intra-module response times are possible by increasing the pump rate or changing the module design.

Two independently controlled fluid flows are supported by each module. Ports 1 and 2 are connected to a dedicated pump structure creating an isolated intra-module flow for mixing and transport of nutrients to the tissue. Continuous re-circulating flow perfusing the hepatocytes tissue scaffold provides the required oxygen and nutrients to maintain the hepatocytes in the liver module. Re-circulating flow on the basolateral side of the airway cells baths the cells in nutrients and enhances mixing. Port 3 is connected to inter-module fluidic plate pump structures via a stainless steel tube creating fluid flow between organs to support tissue interactions. Both infusion and withdrawal of media occurs through Port 3 intermittently during inter-module interactions. This arrangement was chosen to maximize the number of organs supported by the available actuators and is not a fundamental requirement of the system. This arrangement does however impose some operational limitations on organ interactions. Given a finite intra-module mixing time, newly introduced fluid needs time to be convectively transported away from the stainless steel port prior to withdrawing fluid to avoid infusing and withdrawing the same fluid aliquot. The minimum time between infusing and withdrawing an aliquot of fluid is governed by the aliquot volume and introduction rate, the intra-module flow rate, and the module volume. A minimum condition was set to withdraw less than 5% of newly transferred fluid and finite element modeling was use to select operational parameters that achieved this criteria with the interaction scheme described in the Methods section.

Port 3 also controls the module media volume by virtue of the height of the distal end of the stainless steel tubing above the module floor. For each module, the ratio of the number of withdrawing pump cycles to the number of infusing pump cycles is set to a value greater than 1. This pump bias ratio is programmable and its value is set to be greater than the variation in individual pump's stroke volume thus ensuring fluid does not accumulate in any one module in the system on average. The media volume within a module does vary over time due to the dynamic surface tension driven interactions between the culture media and the distal end of the stainless steel tubing; the fluid meniscus repeatedly wets the stainless steel tube during infusions and breaks off during withdrawals. The variation in volume will be dictated by several variables including the media surface tension, the stainless steel tube diameter, and the module media surface area. Direct measurements of the module volumes suggest the media volume height varies plus or minus 0.5 mm above the module floor equating to instantaneous volume changes of less than plus or minus 20% of the median volume for the tissue modules. The circulatory module's volume can potentially vary by the sum of the individual tissue module's volumes and is sized accordingly.

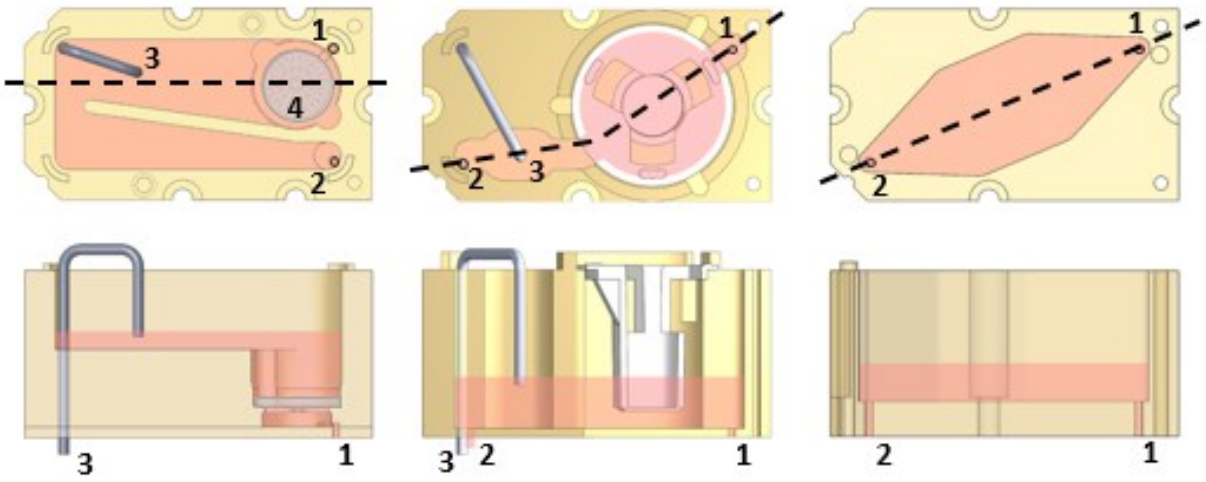

Figure 1s. Plan (top) and section (bottom) views of organ modules. From left to right: liver, airway, and circulation modules. Numeric labels 1 and 2 are intra-module fluidic connection ports while 3 denotes the inter-module fluidic connection, which flows through a stainless steel tube. Note: module ports are sealed to fluidic plate ports via O-rings not shown. Label 4 in the liver module is the hepatocyte scaffold, also shown schematically in the inset at left.

Table 1s. Media volumes in MPS Modules. *In vivo* ratio of Hepatocytes/Normal Human Bronchial Epithelial (NHBE) cells=28.5, Platform Ratio of Hepatocytes/NHBE cells = 1.5, implying that the NHBE cells are over-represented by 19 times in the platform experiments. *In vivo* blood volume is approximately 4850 ml (for a 70 Kg human). This translates to a media/blood volume per cell *in vivo* of 16 pL/hepatocyte and 461 pL/NHBE cell compared to 15,400 pL/hepatocyte and 92,500 pL/cell for the NHBE cells on the platform, resulting in dilution factors of 950 and 200 respectively.

Module	**Volume (ml)**	**Seeded Cells**	**In Vivo Organ**
Mixer	2.0		
Liver	2.0	6×10^5 Hepatocytes 6×10^4 Kupffer	3×10^{11} Hepatocytes
Airway #1	1.5	10^5 NHBE	1.05×10^{10} NHBE
Airway #2	1.25	10^5 NHBE	1.05×10^{10} NHBE
Airway #3	1.25	10^5 NHBE	1.05×10^{10} NHBE
Airway #4	1.25	10^5 NHBE	1.05×10^{10} NHBE

Table 2s. Summary of duty cycle for normal operation of the microphysiological systems platform, comprising a liver module, four airway modules, and a mixer module. For each interaction, the module volume in mL is provided in the second column. The columns that follow contain the interaction ratios and the amount of mixing (in turnovers per hour.) The interaction and self-circulation volumes are provided in the next two columns (in mL/day.) Next, the interaction average flow and self-circulation average flow are provided; note

that the liver module requires 1 uL/sec continuously for oxygenation purposes. Finally, the interaction cycle volume (in mL) is provided in the last column.

	Module Volume [mL]	Interaction Ratios	Mixing: Turnovers/hr	Interaction Volume [mL/day]	Self_Circ_ Volume [mL/day]	Interaction Avg Flow [uL/sec]	Self-Circ Avg. Flow [uL/sec]	Interaction Cycle Volume [mL]
Liver-via-Airway #1	2	0.50	1.8	5.0	86.4	0.06	1.00	0.12
Liver-via-Hepatic	2.00	0.3	1.8	3.0	86.4	0.03	1.00	0.12
Airway #1	1.5	0.5	1.8	5.0	64.8	0.06	0.75	0.12
Airway #2	1.25	0.1	1.8	1.0	54	0.01	0.63	0.12
Airway #3	1.25	0.1	1.8	1.0	54	0.01	0.63	0.12
Airway #4	1.25	0	0	0.0	0	0.00	0.00	0.12
Mixer	2	1.00	1.8	10.0	86.4	0.12	1.00	0.192
Total				10.0	345.60	0.17	3.00	

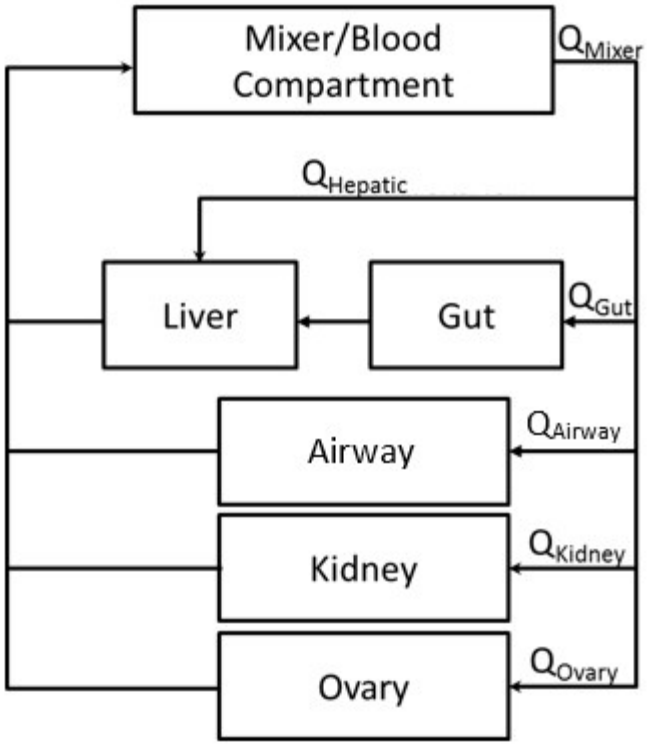

Figure 2s. Five organ fluidic circuit connecting organ modules in a series/parallel configuration. In the experiments presented herein, Gut, Kidney, and Ovary tissues were replaced with airway tissues. Q is the flow rate and the relative rates presented herein, Q_{Gut}=0.5* Q_{Mix}, $Q_{Hepatic}$=0.3* Q_{Mix}, Q_{Airway}=0.1* Q_{Mix}, Q_{Kidney}=0.1* Q_{Mix}, Q_{Ovary}=0.0* Q_{Mix}, and Q_{Mix}= Q_{Gut}+ $Q_{Hepatic}$ + Q_{Airway} + Q_{Kidney} + Q_{Ovary}.

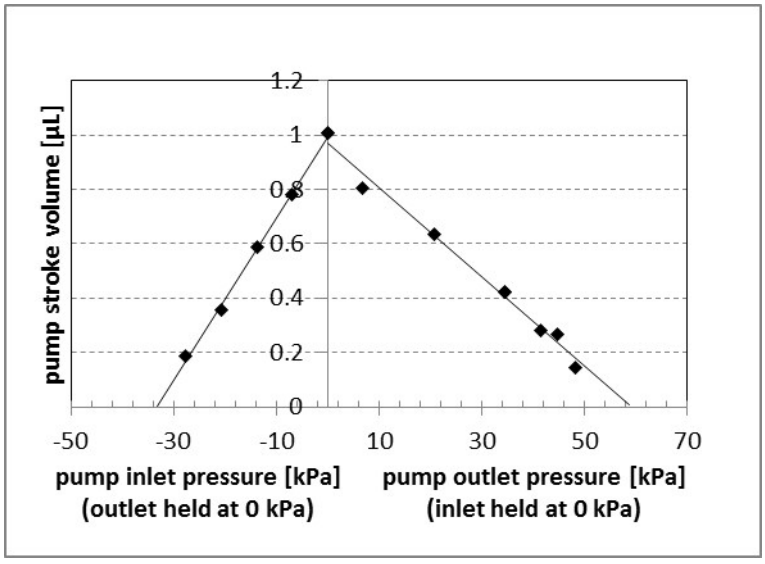

Figure 3s. Pump stroke volume versus applied pressure at 2 Hz pump frequency.

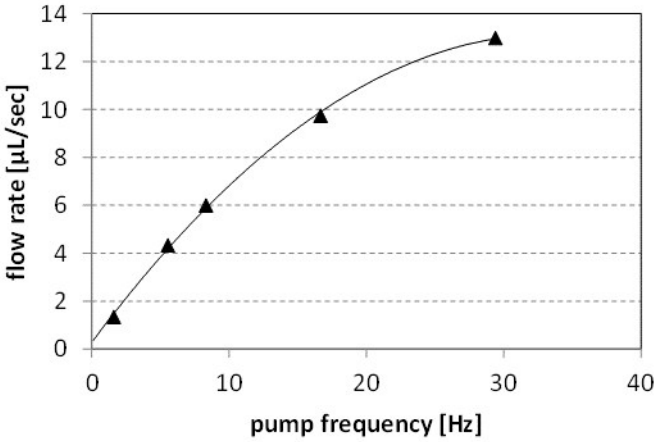

Figure 4s. Pump flow rate versus pump frequency at no load (0 kPa applied pressure).

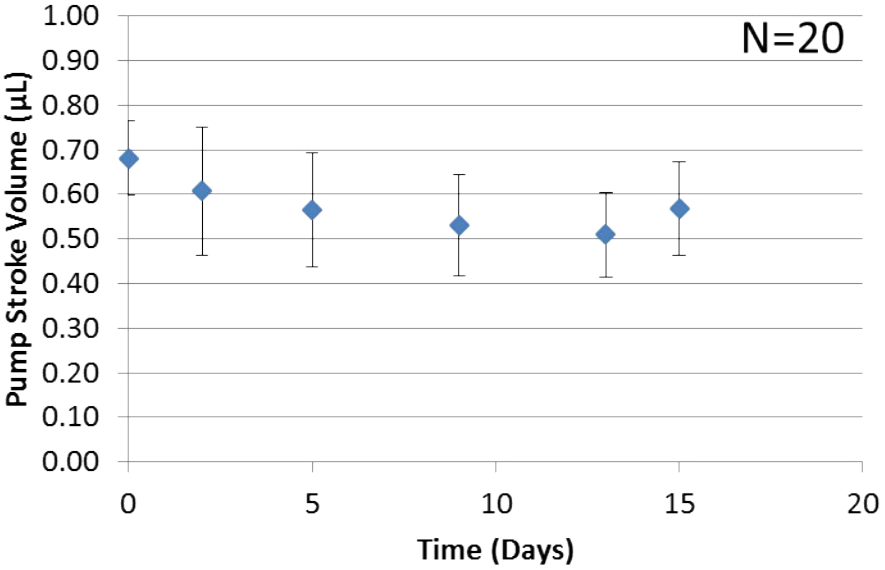

Figure 5s. Flow rates of each platform pump over two week study. Stroke volumes were measured periodically by emptying each module and measuring the volume of fluid transferred after 100 pump cycles either within a module or between modules depending on the respective pump. The overall average stroke volume over two weeks is 0.58 µL with a standard deviation of 0.124 µL. A slight downward trend is observed over time which may be attributed to pump membrane creep causing a relaxation in the restoring force and a dimpled initial position both of which will decreasing the pump volume. Note, the Day 15 data point was taken after the actuators were removed from the fluidic plate for inspection and then re-assembled. Apparently this caused the membrane to partially recover its initial position resulting in an increase in the average stroke volume. Note, these trends match the expected physics, however, the trends are not statistically significant.